Supporting Information

Microscale screen printing of large-area arrays of microparticles for the fabrication of photonic structures and for optical sorting

Mark A. Rose,[a]† T. P. Vinod,[ac]† and Stephen A. Morin*[ab]

[a] Dept. of Chemistry, University of Nebraska-Lincoln, Hamilton Hall, Lincoln, NE 68588, United States
[b] Nebraska Center for Materials and Nanoscience, University of Nebraska-Lincoln, Lincoln, NE 68588, United States
[c] Department of Chemistry, CHRIST (Deemed to be University), Hosur Road, Bengaluru 560029, India.
† Contributed equally to this work

1. Materials

Sylgard® 184 silicone elastomer kit (Dow Corning), Ecoflex® 00-30 (Smooth-On, Inc.), polycarbonate film (McMaster-Carr®), polyethylene terephthalate (McMaster-Carr®), microscope glass slides (Thermo Fisher Scientific), thermoplastic polyurethane (Elastollan® soft 45A, BASF), microparticles based on polystyrene (sizes 20 μm and 30 μm, Sigma Aldrich), Polybead® polystyrene 2.0 micron microspheres (Polysciences), 1H, 1H, 2H, 2H-perfluorooctyltrichlorosilane (Oakwood Chemical, CAS 78560-45-9), ethanol (200 proof, Decon Laboratories), SU-8 2050 (MicroChem), SU-8 developer (MicroChem), Lens Bond optical cement (polyurethane, Summers optical), silica gel (Sigma Aldrich, CAS 112926-00-8), glass spheres (Sigma Aldrich, CAS 65997-17-3), iron (II) chloride tetrahydrate (Thermo Fisher Scientific, CAS 13478-10-9), iron (III) chloride hexahydrate (Sigma Aldrich, CAS 10025-77-1), ammonium hydroxide (Thermo Fisher Scientific, CAS 1336-21-6), hydrochloric acid (Thermo Fisher Scientific, CAS 7647-01-0), and sea sand (Thermo Fisher Scientific, CAS 14808-60-7)

were obtained from the indicated suppliers and used without further purification. Water soluble tape was obtained from Aquasol Welding.

2. Preparation of MIMIC masks

PDMS stamps were prepared through standard soft lithography procedures. These stamps were placed on a clean glass slide with the posts (protruding parts) of the stamps in contact with the glass surface. A drop of optical cement (polyurethane) was placed at the edge of the stamp/glass interface. The viscous liquid of optical cement was allowed to fill inside the vertical gaps through capillary action, followed by irradiation with UV light (40 mW/cm^2,75s). The PDMS stamp was peeled off and then the MIMIC mask was detached from the surface with the help of a razor blade. The mask was consisting of openings corresponding to the position and size of the posts in the PDMS stamp.

3. Preparation of Particles

The polystyrene solutions were made by centrifuging 200 μL of 10% polystyrene down and then re-dispersed in 1 mL of water. This centrifuging process was repeated three times to thoroughly wash the particles. Finally the polystyrene spheres were suspended in 1 mL of either ethanol or water. The iron oxide particles (Fe_3O_4) were prepared and washed using a previous procedure[1] and suspended in ethanol for patterning. The sand and silica gel were both too big to be suspended and were introduced to the surface while they were dry.

4. Deposition of particles through the MIMIC mask

The MIMIC mask was placed on the substrate. Conformal contact was ensured by pressing the mask down with mild and uniform force. Few drops of a solution of the microparticles (typically

2% wt solution in ethanol) were dropped on the mask and dried at 80°C. The dry film of particles formed was spread evenly by rubbing (with mild force) in one direction using an Al SEM sample holder (sometimes containing a flat piece of Teflon attached to the bottom). A flat solid surface covering the whole mask area was made in contact with the mask and mechanical pressure was applied downwards. This resulted in the deposition of microparticles through the openings in the mask.

5. Calculating the effectiveness of the patterning

We looked at three different statistics to quantify the efficiency of our patterns: yield, accuracy, and efficiency. We calculated yield of the pattern by comparing the ratio of filled mask holes versus total number of mask holes. The process of removing the mask could cause a shift in the location of the particles. Thus we calculated the accuracy of the patterning by overlaying an image of the particles with an image of the mask aligning the particles and masks through visual observation. We then looked at the ratio of the area of the particles inside the mask area versus the total area of the particles using ImageJ (National Institutes of Health). Finally, we examined efficiency by taking the area of particles inside the mask area (just like above) divided by the maximum area of the particles that can be patterned (since we have 160 - 40x40 μm wells that can only fit 1 – 30 μm this number would be 113,094 μm^2). We used the efficiency metric to ultimately determine the effectiveness of our patterns because in order to get high efficiency values a surface must have both high yield and accuracy values.

6. Bonding of assembled particles and release of monolithic structures

Particle assembled through MIMIC mask were bonded together with solvent vapor annealing. After assembling the particles on the substrate of interest, the substrate was moved into a beaker containing acetone. The substrate was placed on a support so that it was not directly touching the

liquid. The beaker was then closed and kept at room temperature for 1 h, which facilitated the annealing of particles with acetone vapor. The monolithic assemblies thus formed could be released from the substrate using a water soluble tape. The tape is made in contact with the assembled structures and then removed from the surface. Free standing monolithic structures were obtained by dissolving the tape by treatment with water.

7. Calculating the expected number of particles in a well

We used Wolfram Alpha[2] to calculate many of the expected number of particles in a well. The following equations could also be utilized in order to calculate the number of particles.

$$\text{side length} = 4 \times \text{radii} \qquad \text{eqn. 1}$$

$$\text{side length} = 6 \times \text{radii} \qquad \text{eqn. 2}$$

$$\text{side length} = 5.464 \times \text{radii} \qquad \text{eqn. 3}$$

$$\text{side length} = 9.464 \times \text{radii} \qquad \text{eqn. 4}$$

$$\text{side length} = 15.7 \times \text{radii} \qquad \text{eqn. 5}$$

$$\text{long diagonal} = 5.154 \times \text{radii} \qquad \text{eqn. 6}$$

$$\text{radius} = 8.96 \times \text{radii} \qquad \text{eqn. 7}$$

Where each equation calculates the smallest polyhedral needed to hold a set number of circles. Equation 1 calculates the side length of a square needed to pack 4 circles. Equation 2 calculates the side length of a square needed to pack 9 circles. Equation 3 calculates the side length of an equilateral triangle needed to pack 3 circles. Equation 4 calculates the side length of an equilateral triangle needed to pack 10 circles.[3] Equation 5 calculates the side length of an equilateral triangle needed to pack 28 circles.[4] Equation 6 calculates the long diagonal length of a hexagon needed to pack 19 circles. Equation 7 calculates the radius of a circle needed to pack 64 circles.

8. Interaction energies between substrates with particles

We calculated the Hamaker constant between two substances across a medium (A_{132}) by utilizing equation 8.

$$A_{132} = (\sqrt{A_{11}} - \sqrt{A_{33}})(\sqrt{A_{22}} - \sqrt{A_{33}}) \qquad \text{eqn. 8}$$

Where A_{ii} is the Hamaker constant of a material interacting with itself, 1 is the surface of the first material, 2 is the surface of the second material, and 3 is the medium. We used the Hamaker constants (A_{ii}) found in literature for PDMS (4.4×10^{-20} J), silica (6.5×10^{-20} J), polystyrene (6.5×10^{-20} J), and silicon (1.8×10^{-19} J).[5,6] In order to approximate the other surfaces we related the surface energy of a substrate to the Hamaker constant using equations 9 – 11.[5]

$$W = \frac{-A_{11}}{12 \times \pi \times D_o^2} \qquad \text{eqn. 9}$$

$$W = -2\gamma \qquad \text{eqn. 10}$$

$$A_{11} = 24 \times \pi \times D_o^2 \times \gamma \qquad \text{eqn. 11}$$

Where D_o is the equilibrium distance between two identical materials (0.16 nm)[7] and γ is the surface energy. We used the surface energy of PET (0.0446 J/m^2), PC (0.0342 J/m^2), Parafilm (0.0286 J/m^2),[8] thermoplastic polyurethane (0.0378 J/m^2),[9] and Ecoflex (0.03515 J/m^2)[10] found in literature in order to calculate their Hamaker constants. We used the Hamaker constants in order to calculate the interaction energy between all the substrates used and polystyrene using equation 4 in the main text.

We accounted for the adhesion mechanics using the JKR theory,[11] which meant we needed to calculate the interaction energy per unit area. We calculated this using equation 12, which shows the interaction energy of a flat surface interacting with a flat surface.

$$E = \frac{-A_{132}}{12\pi D^2} \qquad \text{eqn. 12}$$

Where E is the interaction energy per unit area, A_{132} is the Hamaker constant, and D is the equilibrium distance between two materials (0.2 nm). We used the interaction energy per unit area along with elastic moduli (found in technical brochures or in literature)[12] in order to calculate the contact radius of the particle with different surfaces under zero load (equation 5 in the main text and SI table 2). Finally using the contact radius of the particle we converted that to the contact area (A) which we used to find the actual interaction energy of PS with each substrate.

Creating far field interference pattern

We captured the far field interference pattern by shining a laser pointer through the patterned region of a 2D photonic crystal. The interference pattern was projected onto a flat white wall and captured using Nikon D5100. When the pattern was very close to the image plane the only interference pattern observed was concentric circles which indicates a polycrystalline HCP lattice (Fig. 4h). As the pattern was moved farther from the image plane the square lattice of the patterned vacancies are observed (Fig. i, j). When we imaged the far field interference pattern of the complimentary pattern on the tape we were only able to observe the square lattice. We believe this was due to the small amount of particles transferred which lead to a very small diffraction pattern that we did not see.

References

1. T. P. Vinod, J. H. Chang, J. Kim and S. W. Rhee, *Bull. Korean Chem. Soc.*, 2008, **29**, 799-804.
2. Wolfram Alpha, https://www.wolframalpha.com/examples/mathematics/geometry/packing-and-covering-problems/geometric-packing-in-2d/, (accessed May 2018).
3. N. Oler, *Canad. Math. Bull.*, 1961, **4**, 153-155.
4. K. J. Nurmela, *Exp. Math.*, 2000, **9**, 241-250.
5. J. N. Israelachvili, *Intermolecular and Surface Forces, 3rd Edition*, 2011.
6. L. Bergstrom, *Adv. Colloid Interface Sci.*, 1997, **70**, 125-169.
7. V. Medout-Marere, *J. Colloid Interface Sci.*, 2000, **228**, 434-437.
8. B. Janczuk and T. Bialopiotrowicz, *J. Colloid Interface Sci.*, 1989, **127**, 189-204.
9. T. G. Vargo, D. J. Hook, J. A. Gardella, M. A. Eberhardt, A. E. Meyer and R. E. Baier, *J. Polym. Sci. A*, 1991, **29**, 535-545.
10. J. W. Rhim and S. I. Hong, *Food Sci. Biotechnol.*, 2007, **16**, 234-237.
11. K. L. Johnson, K. Kendall and A. D. Roberts, *Proc. Royal Soc. A*, 1971, **324**, 301-313.
12. J. J. Bowen, J. M. Taylor, C. P. Jurich and S. A. Morin, *Adv. Funct. Mater.*, 2015, **25**, 5520-5528.
13. D. Chicot, J. Mendoze, A. Zaoui, G. Louis, V. Lepingle, F. Roudet, J. Lesage, *Mater. Chem. Phys.,* 2011, **129,** 862-870
14. B. Faure, G. Salazar-Alvarez, and L. Bergstrom, *Langmuir*, 2011, **27,** 8659-8664

Material	K (MPa)[a]	ϒ (J/m^2)[b]	A_{ii} (10^{-20} J)[c]	% Transmittance (Visible region)	Refractive Index (η)	Magnetic
PS	2,800	N/A	6.5	N/A	1.5915	No
Silica	70,000	N/A	6.5	> 90%	1.544	No
Fe_3O_4	200,000	N/A	4.3	N/A	2.3438	Yes
PDMS	1.32	N/A	4.4	> 90%	1.4118	No
Parafilm	45	0.0286	5.5	50% < % T > 70%	1.442	No
TPU	25	0.0378	7.3	35% < % T > 90%	N/A	No
Ecoflex 00-30	0.0689	0.03515	6.8	20% < % T > 45%	N/A	No
PET	2,300	0.0446	8.6	80% < % T > 90%	1.575	No
PC	2,600	0.0342	6.6	85% < % T > 95%	1.5846	No
Silicon	160,000	N/A	18	0%	N/A	No

[a] Technical documents from manufacturer and Ref. 12 – 13
[b] Ref. 7 – 10
[c] Ref. 5, 6, and 14

Table S1. Physical properties of materials used in this study.

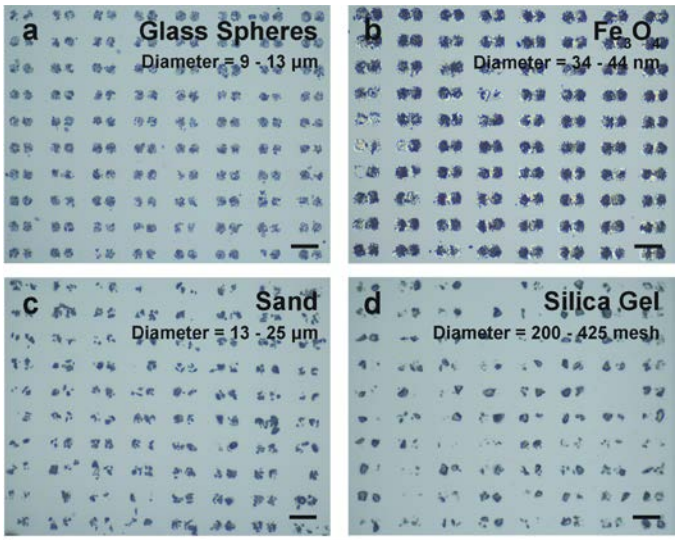

	Yield	Accuracy	Efficiency
Glass Spheres	100%	88%	79%
Fe_3O_4	99%	77%	82%
Sand	94%	80%	48%
Silica Gel	80%	80%	54%

Figure S1. µSP of different materials: (a) glass spheres, (b) Fe_3O_4 nanoparticles, (c) sand, (d) silica gel. All scale bars are 100 µm.

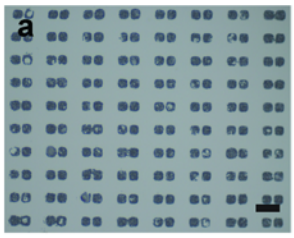

Polystyrene particles
PDMS substrate
b_{hole} = 40 ± 2 µm
d_{part} = 2 µm
$n_{expected}$ = 444
Avg n = 400 ± 60

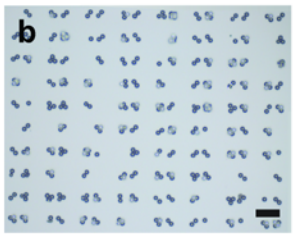

Polystyrene particles
PDMS substrate
b_{hole} = 40 ± 2 µm
d_{part} = 20 ± 0.3 µm
$n_{expected}$ = 3
Avg n = 2 ± 1

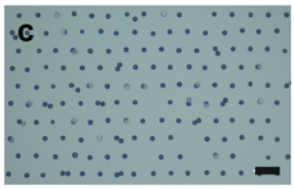

Polystyrene particles
PDMS substrate
r_{hole} = 30 µm
d_{part} = 20 µm
$n_{expected}$ = 1
Avg n = 1.0 ± 0.4

	Yield	Accuracy	Efficiency
2 µm PS - dimer	100%	86%	89%
20 µm PS - dimer	88%	89%	68%
20 µm PS - single	94%	93%	96%
30 µm PS - dimer	98%	89%	96%

Figure S2. µSP of different sized PS particles onto PDMS. (a) Optical image of 2 µm PS particles patterned through 40 µm square holes. (b) Optical image of 20 µm PS particles patterned through 40 µm square holes. (c) Optical image of 20 µm PS particles patterned through 30 µm diameter circular holes arranged in a hexagonal array with spacing of 60 µm. (d) Tabulated metrics including data for 30 µm diameter particles (main text Fig 1). Scale bars are 100 µm.

Substrate 1	Medium	Substrate 2	A_{132} (J)	E_{132} (J)	Efficiency Rank
PDMS	Air	Polystyrene	5.35E-20	-6.68E-16	1
Parafilm	Air	Polystyrene	5.99E-20	-7.49E-16	2
TPU	Air	Polystyrene	6.89E-20	-8.61E-16	3
Ecoflex	Air	Polystyrene	6.78E-20	-8.48E-16	4
PET	Air	Polystyrene	7.48E-20	-1.25E-15	5
Glass	Air	Polystyrene	6.50E-20	-8.13E-16	6
PC	Air	Polystyrene	6.55E-20	-8.19E-16	7
Silicon	Air	Polystyrene	1.08E-19	-1.35E-15	8

Table S2. Calculated values for Hamaker constants (A_{132}) and interaction energy of a sphere and a flat substrate (E_{132}).

Substrate	E (J/m^2)	A_0 (m)	E_{132} (J)	Efficiency Ranking
PDMS	-0.03547	3.80E-17	-1.61E-34	1
Parafilm	-0.03972	1.25E-18	-1.94E-37	2
TPU	-0.04567	2.58E-18	-9.57E-37	3
Ecoflex 00-30	-0.04499	9.23E-16	-1.20E-31	4
PET	-0.04961	3.05E-20	-1.45E-40	5
Silica	-0.04311	8.71E-22	-1.03E-43	6
PC	-0.04344	2.36E-20	-7.61E-41	7
Silicon	-0.07173	6.34E-22	-9.05E-44	8

Table S3. Calculated interaction energies (E_{132}) of polystyrene spheres with reported substrates using the JKR theory which used the elastic modulus (K), interaction energy per unit area (E), and contact area (A_0).

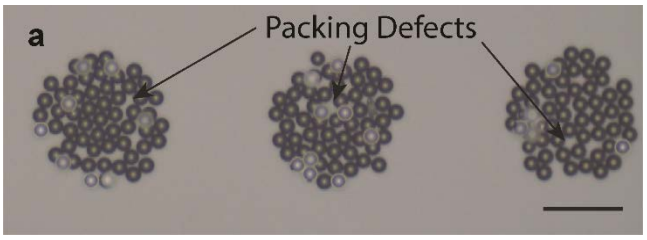

Figure S3. Packing defects present in large circle pattern. Scale bar is 100 μm.

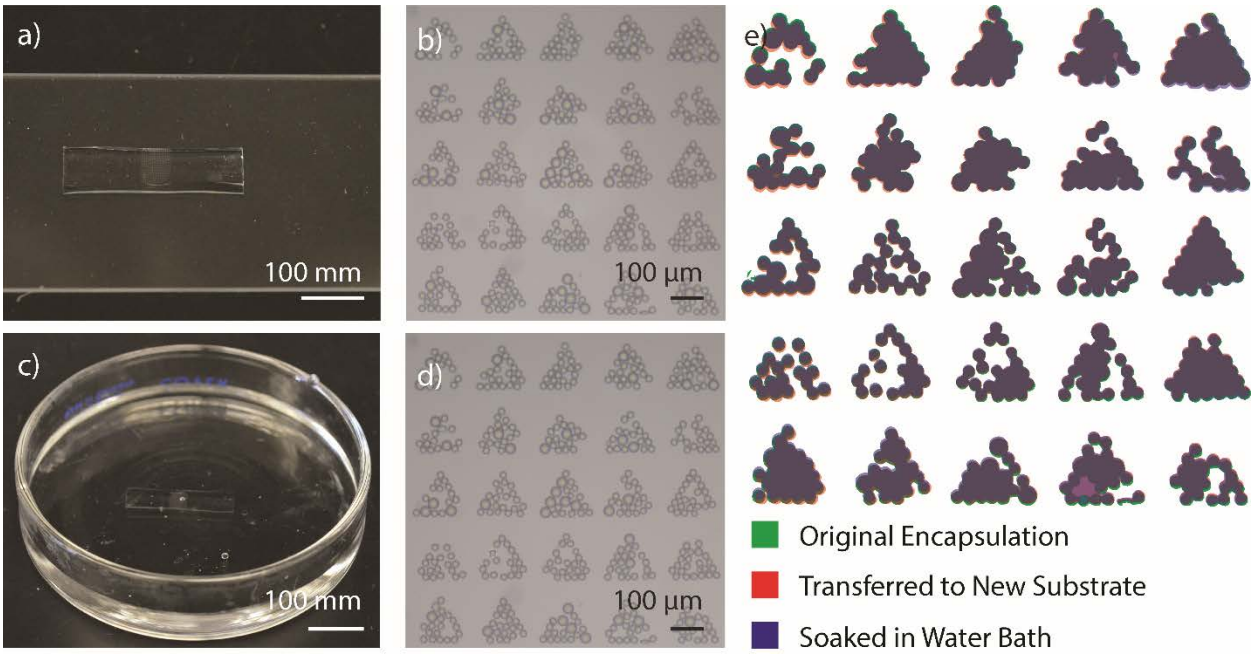

Figure S4. Testing the encapsulation of the barcode. (a, b) Barcode has been encapsulated in PDMS and moved from original substrate. (c, d) Barcode has been encapsulated in PDMS and soaked in a water bath for 5 min. (e) Overlay of the 25 well array with the original encapsulated array (green), the array that had been moved to a new substrate (red), and the array that had been soaked in water (blue).